Supporting Information

for

Rational Design of a Structural Framework with Potential Use to Develop Chemical Reagents That Target and Modulate Multiple Facets of Alzheimer's Disease

Sanghyun Lee,[1,ξ] Xueyun Zheng,[2] Janarthanan Krishnamoorthy,[3,4] Masha G. Savelieff,[1] Hyun Min Park,[1,5] Jeffrey R. Brender,[3,4] Jin Hoon Kim,[1,5] Jeffrey S. Derrick,[4] Akiko Kochi,[4] Hyuck Jin Lee,[4] Cheal Kim,[5] Ayyalusamy Ramamoorthy,[3,4,*] Michael T. Bowers,[2,*] and Mi Hee Lim[1,4,6,*]

[1] Life Sciences Institute, University of Michigan, Ann Arbor, Michigan 48109-2216, USA

[2] Department of Chemistry and Biochemistry, University of California, Santa Barbara, California 93106-9510, USA

[3] Biophysics, University of Michigan, Ann Arbor, Michigan 48109-1055, USA

[4] Department of Chemistry, University of Michigan, Ann Arbor, Michigan 48109-1055, USA

[5] Department of Chemistry, Seoul National University of Science and Technology, Seoul 139-743, Korea

[6] School of Nano-Bioscience and Chemical Engineering, Ulsan National Institute of Science and Technology (UNIST), Ulsan 689-798, Korea

[ξ] Present address: Department of Molecular and Cellular Biology, University of Guelph, Guelph, Ontario N1G 2W1, Canada

* To whom correspondence should be addressed: ramamoor@umich.edu, bowers@chem.ucsb.edu, and mhlim@unist.ac.kr

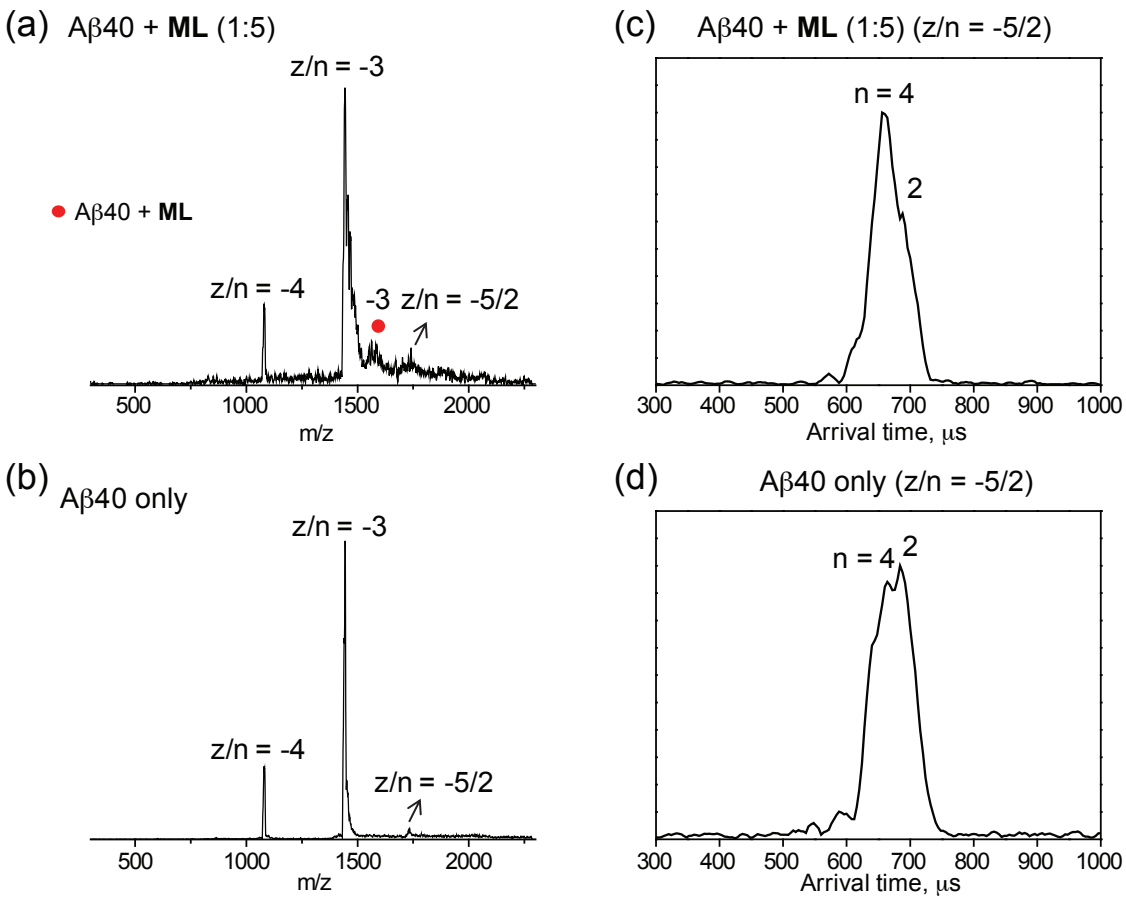

Figure S1. Interaction and effect of **ML** on Aβ40 (Aβ:**ML** = 1:5). (a and b) Mass spectra of Aβ40 with and without **ML**, where z/n is charge/oligomer ratio. (c and d) The ATD of –5/2 Aβ40 in the presence and absence of **ML**. Oligomer number (n) is noted for each feature.

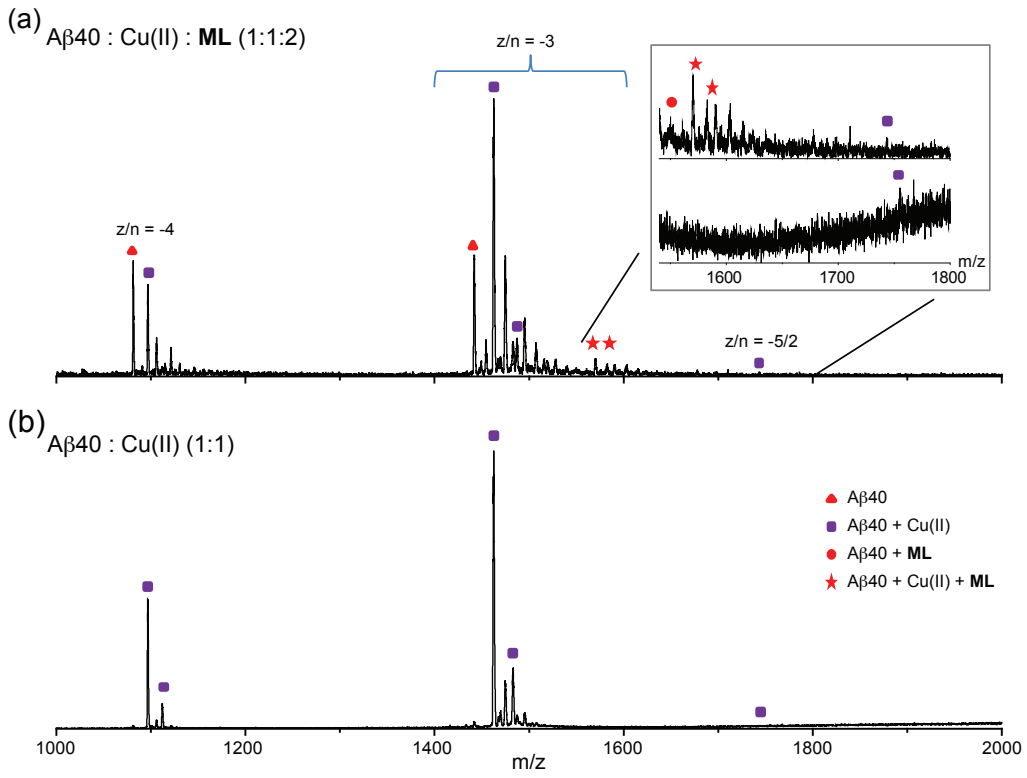

Figure S2. Mass spectra of samples containing Aβ40 and Cu(II) in the absence and presence of **ML**. (a and b) Mass spectra of a mixture of Aβ40:Cu(II):**ML** (1:1:2) and Aβ40:Cu(II) (1:1). The peaks for Aβ40, Cu(II)-bound Aβ40, **ML**-bound Aβ40, and complexes of Aβ40, Cu(II), and **ML** are labeled according to the legend.

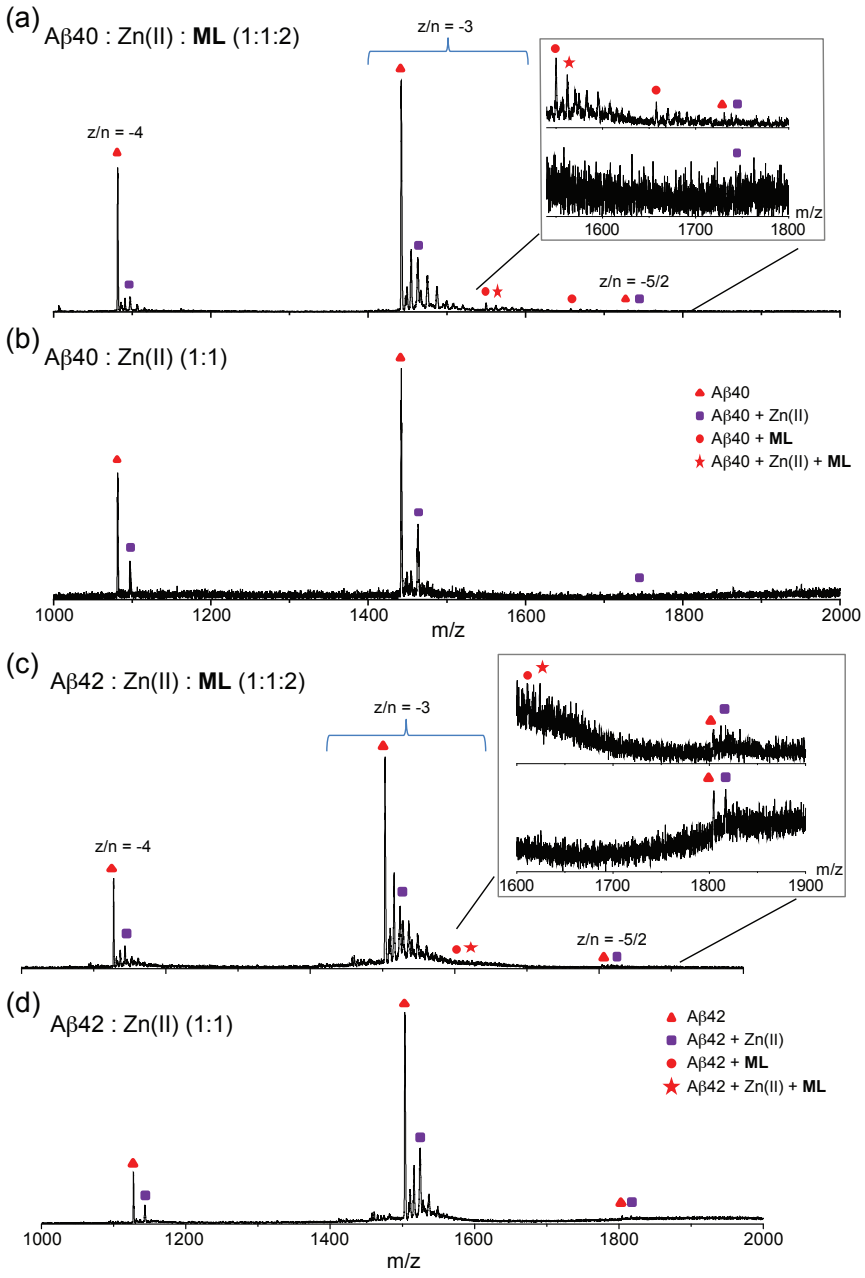

Figure S3. Mass spectra of Zn(II)–Aβ40/42 samples with and without **ML**. Mass spectra of a mixture of Aβ40/42:Zn(II):**ML** (1:1:2, a and c) and Aβ40/42:Zn(II) (1:1, b and d). The peaks for Aβ40/42, Zn(II)-bound Aβ40/42, **ML**-bound Aβ40/42, and complexes of Aβ40/42, Zn(II), and **ML** are labeled according to the legend.

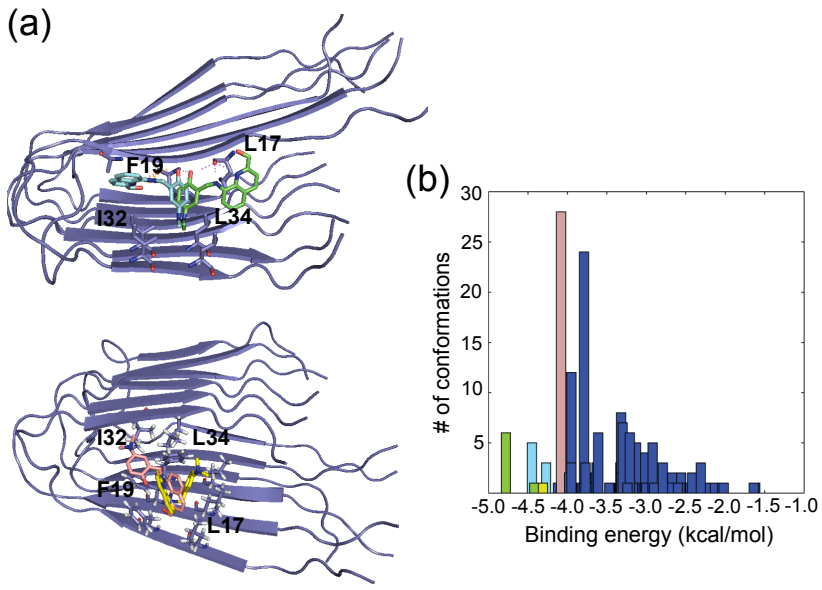

Figure S4. Docking of **ML** to negatively staggered Aβ40 fibers (PDB 2LMO). (a) Lowest four energy conformations of **ML** to Aβ40 fibers. (b) Cluster energy analysis of **ML** binding to Aβ40 fibers. The lowest six energy conformations are color-coded to match the conformations shown in (a). Matching colors indicate conformations closely related by symmetry.

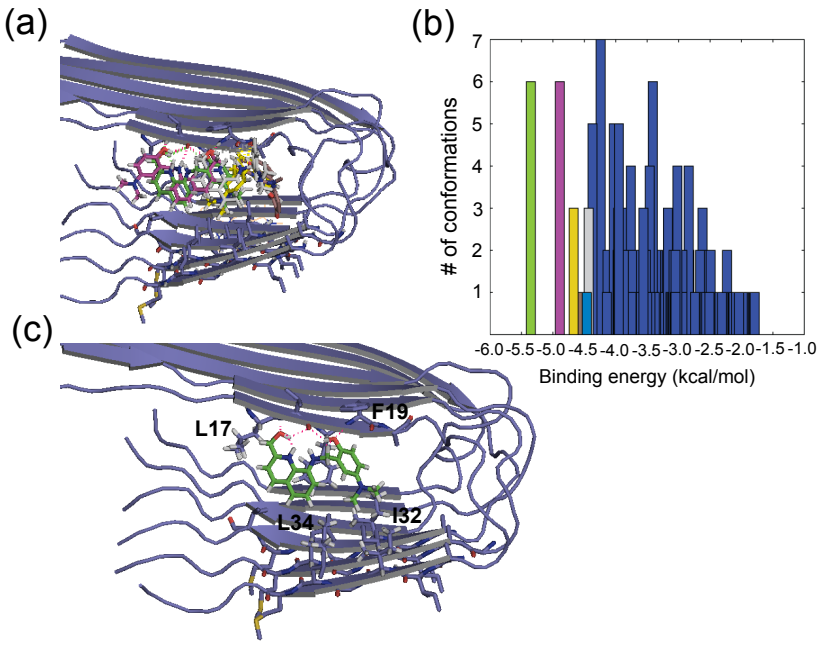

Figure S5. Docking of **ML** to positively staggered Aβ40 fibers (PDB 2LMN). (a) Lowest six energy conformations of **ML** to Aβ40 fibers. (b) Cluster energy analysis of **ML** binding to Aβ40 fibers. The lowest six energy conformations are color-coded to match the structures shown in (a). (c) A close-up of the lowest energy docked conformation.

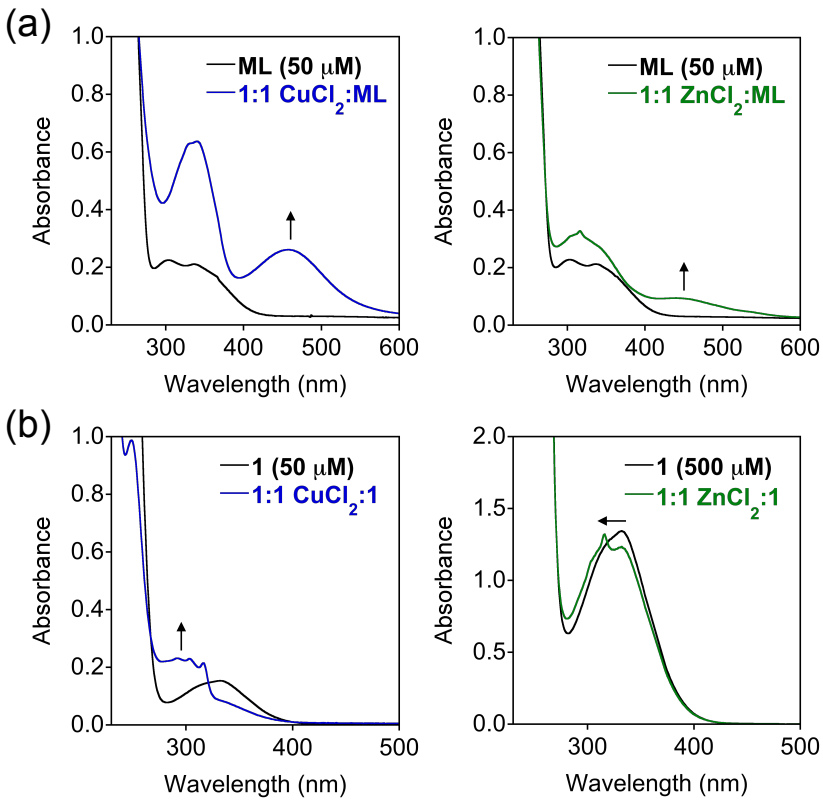

Figure S6. Metal binding studies of **ML** and **1**. (a) UV-Vis spectra of **ML** (black line) and with $CuCl_2$ (left, blue line; 30 min incubation) or $ZnCl_2$ (right, green line; 60 min incubation). (b) UV-Vis spectra of **1** (black line) with $CuCl_2$ (left, blue line; 10 min incubation) or $ZnCl_2$ (right, green line; 10 min incubation). Note that the scale on **1**:$ZnCl_2$ is different to other spectra. Experimental conditions: [M(II)]:[L] = 1:1; 20 mM HEPES, pH 7.4, 150 mM NaCl; room temperature.

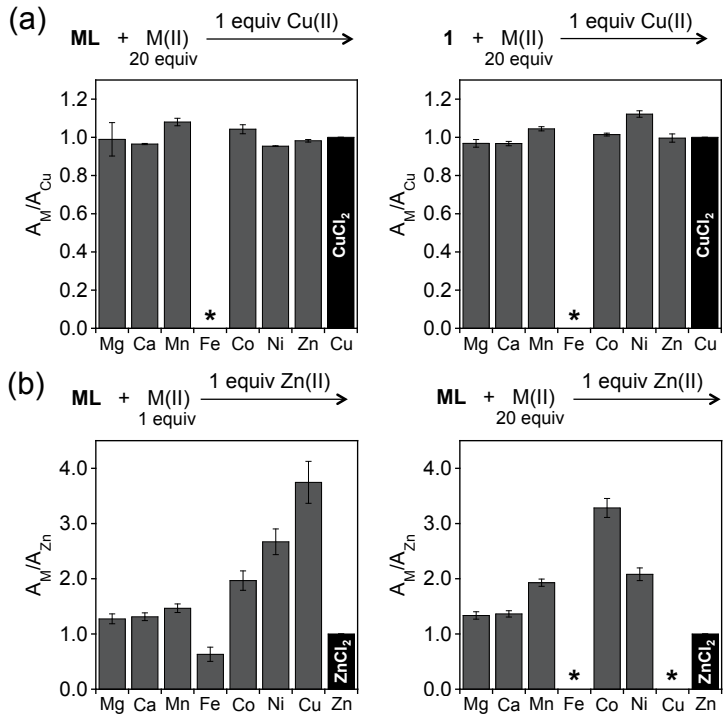

Figure S7. (a) Metal selectivity studies of **ML** and **1** for Cu(II) over other divalent metal ions. Gray bars represent the subsequent addition of $CuCl_2$ (50 μM) to solutions of the ligand with 20 equivalents of other divalent metal ions ($MgCl_2$, $CaCl_2$, $MnCl_2$, $FeCl_2$, $CoCl_2$, $NiCl_2$, and $ZnCl_2$). The absorbance of **ML** and **1** at 485 nm at 291 nm, respectively, was used to calculate A_M/A_{Cu}. (b) Metal selectivity studies of **ML** for Zn(II) over other divalent metal ions. Gray bars represent the subsequent addition of $ZnCl_2$ (50 μM) to solutions of ligand with other divalent metal ions. The absorbance of **ML** at 425 nm was used to calculate A_M/A_{Zn}. Noticeable A_M values at 425 nm were observed upon incubation of some divalent metal ions with **ML**, resulting in $A_M/A_{Zn} > 1$, although Zn(II) is relatively selective over other divalent metal ions (*i.e.*, Mg(II), Ca(II), and Mn(II)). Experimental conditions: [MCl_2] = 50 μM or 1 mM, [$CuCl_2$ or $ZnCl_2$] = 50 μM; 20 mM HEPES, pH 7.4, 150 mM NaCl; 5 or 15 min incubation; room temperature. Due to the limited spectral change, Zn(II) selectivity of **1** was not performed. * Indicates precipitation in the reaction.

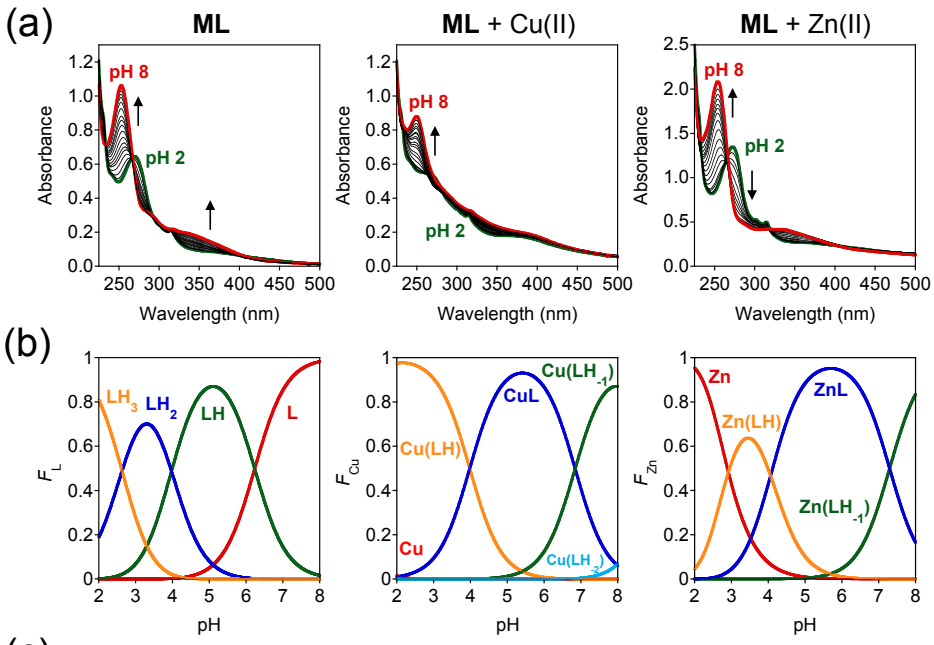

(c)

						pK_a[a]
H_3L	⇌	H_2L	+	H	(pK_{a1})	2.628(5)
H_2L	⇌	HL	+	H	(pK_{a2})	3.971(2)
HL	⇌	L	+	H	(pK_{a3})	6.230(6)

					logβ[a]	
					Cu(II)	**Zn(II)**
M	+	LH	⇌	M(LH)	15.33(1)	11.617(5)
M	+	L	⇌	ML	11.35(1)	7.533(7)
M	+	LH_{-1}	⇌	$M(LH_{-1})$	4.50(1)	0.256(9)
M	+	LH_{-2}	⇌	$M(LH_{-2})$	−4.61(2)	–
pM (= −log[$M_{unchelated}$]; pH 6.6 / 7.4)					11.46 / 12.03	– / 7.88

Figure S8. Solution speciation studies of **ML** with and without Cu(II) or Zn(II). (a) UV-Vis variable-pH titration spectra of **ML** in the absence (left) and presence of Cu(II) (middle) or Zn(II) (right). Note that the y scale on **ML** + Zn(II) is different to other spectra. (b) Solution speciation diagrams (F_L = fraction of compound with given protonation). (c) Summary of acidity constants (pK_a) of **ML** (top) and stability constants (logβ) of Cu(II)–**ML** or Zn(II)–**ML** complexes (bottom). Charges are omitted for clarity. [a] The error of the last digit is shown in parentheses. Experimental conditions: [**ML**] = 50 μM (for metal-free); [M(II)]:[**ML**] = 1:2, [Cu(II)] = 25 μM (incubation with **ML** for 1 h), [Zn(II)] = 50 μM (incubation with **ML** for 2 h); pH 2.0-8.0; I = 0.10 M NaCl; room temperature.

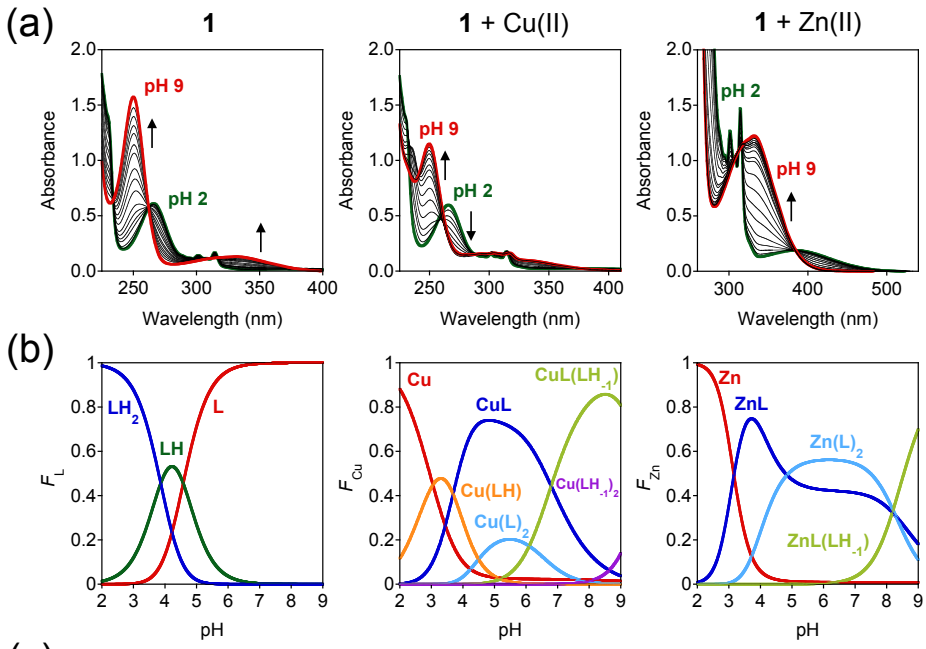

(c)

				pK_a[a]
H_2L	⇌	HL + H	(pK_{a1})	3.866(4)
HL	⇌	L + H	(pK_{a2})	4.58(1)

		logβ[a]	
		Cu(II)	**Zn(II)**
M + LH	⇌ M(LH)	9.90(1)	–
M + L	⇌ ML	6.21(1)	5.635(5)
M + 2L	⇌ $M(L)_2$	10.43(1)	9.725(8)
M + L + LH_{-1}	⇌ $ML(LH_{-1})$	4.33(2)	1.522(9)
M + 2(LH_{-1})	⇌ $M(LH_{-1})_2$	−5.43(2)	–
pM (= −log[$M_{unchelated}$]; pH 6.6 / 7.4)		6.25 / 6.28	– / 5.65

Figure S9. Solution speciation studies of **1** with and without Cu(II) or Zn(II). (a) UV-Vis variable-pH titration spectra of **1** in the absence (left) and presence of Cu(II) (middle) or Zn(II) (right). (b) Solution speciation diagrams (F_L = fraction of compound with given protonation). (c) Summary of acidity constants (pK_a) (top) and stability constants (logβ) of **1** with Cu(II) and Zn(II) (bottom). Charges are omitted for clarity. [a] The error of the last digit is shown in parentheses. Experimental conditions: [**1**] = 50 μM (for metal-free); [M(II)]:[**1**] = 1:2, [Cu(II)] = 25 μM (incubation with **1** for 1 h), [Zn(II)] = 250 μM (incubation with **1** for 2 h); pH 2.0-9.0; I = 0.10 M NaCl; room temperature.

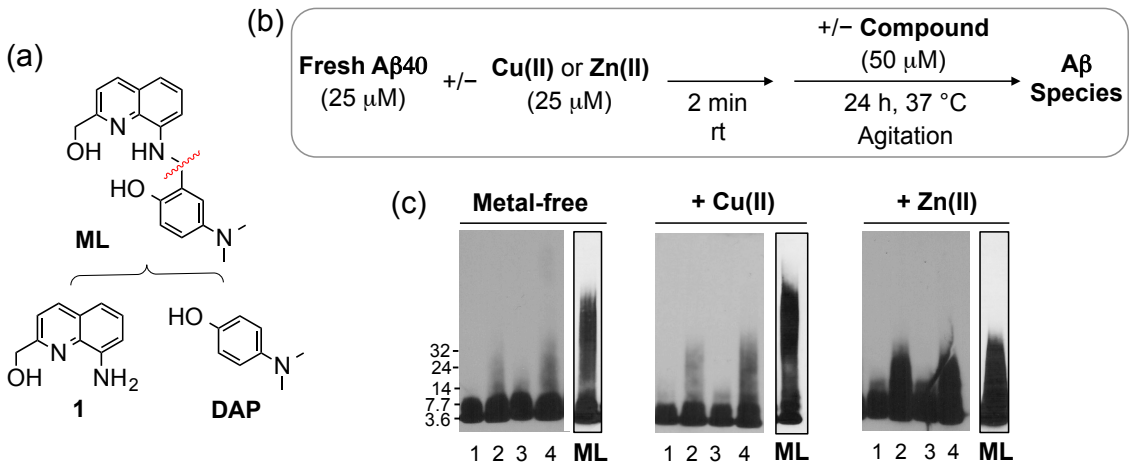

Figure S10. Influence of **1**, **DAP**, or **ML** on the formation of metal-free and metal-induced Aβ40 aggregates. (a) Chemical structures of **1**, **DAP**, and **ML**. (b) Scheme of the inhibition experiment. (c) Aβ species were visualized by gel electrophoresis using immunoblotting with an anti-Aβ antibody (6E10). Experimental conditions: Aβ (25 μM); $CuCl_2$ or $ZnCl_2$ (25 μM); compound (50 μM); 24 h; pH 6.6 (for Cu(II) experiments) or 7.4 (for metal-free and Zn(II) experiments); 37 °C; constant agitation. Lanes: (1) Aβ ± $CuCl_2$ or $ZnCl_2$; (2) Aβ ± $CuCl_2$ or $ZnCl_2$ + **DAP**; (3) Aβ ± $CuCl_2$ or $ZnCl_2$ + **1**; (4) Aβ ± $CuCl_2$ or $ZnCl_2$ + (**DAP** + **1**).

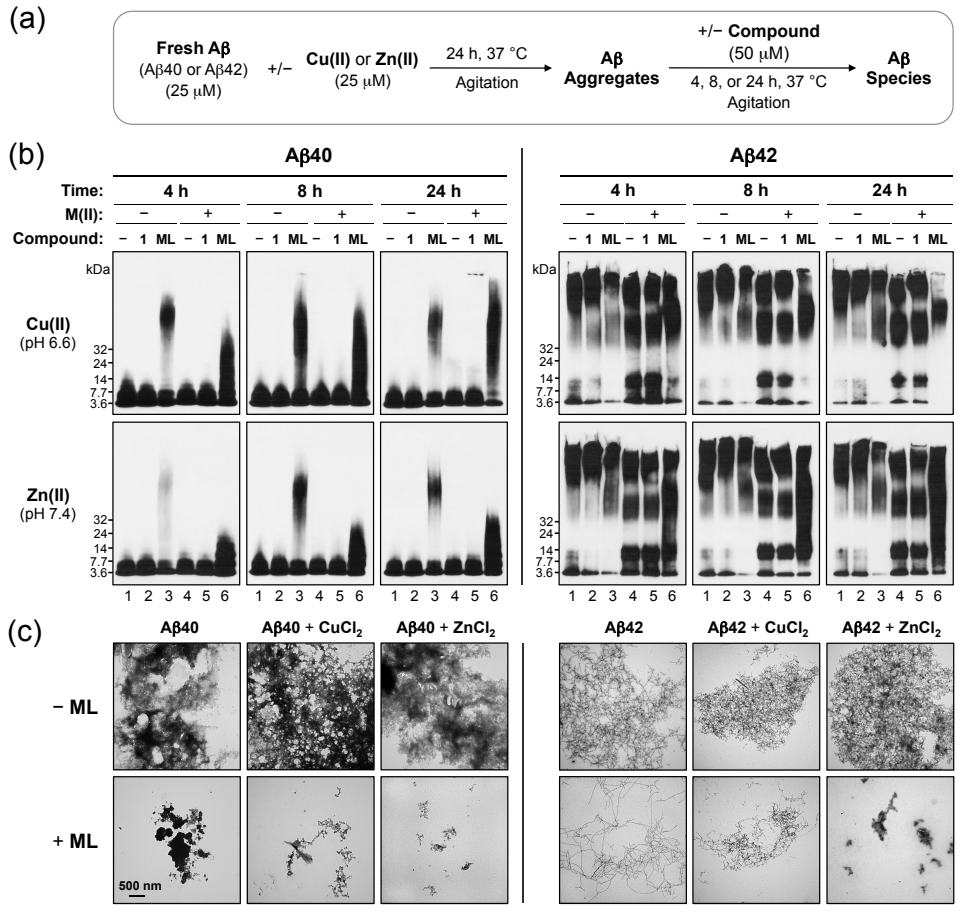

Figure S11. Transformation of preformed metal-free and metal-induced Aβ40/42 aggregates in the presence of **ML** or **1**. (a) Scheme of the disaggregation experiment. (b) Aβ species were visualized by gel electrophoresis using immunoblotting with an anti-Aβ antibody (6E10). Aβ aggregates were produced by incubation of Aβ (25 μM) with/without $CuCl_2$ or $ZnCl_2$ (25 μM) in 150 μM NaCl and 20 μM HEPES, pH 6.6 (for Cu(II) experiment) or pH 7.4 (for metal-free and Zn(II) experiments) at 37 °C with constant agitation for 24 h. **ML** or **1** (50 μM) was then added to each sample and the resulting solutions were incubated an additional 4, 8, or 24 h. Lanes: (1) Aβ; (2) Aβ + **1**; (3) Aβ + **ML**; (4) Aβ + [$CuCl_2$ or $ZnCl_2$]; (5) Aβ + [$CuCl_2$ or $ZnCl_2$] + **1**; (6) Aβ + [$CuCl_2$ or $ZnCl_2$] + **ML**. (c) TEM images from (b) samples following 24 h incubation.

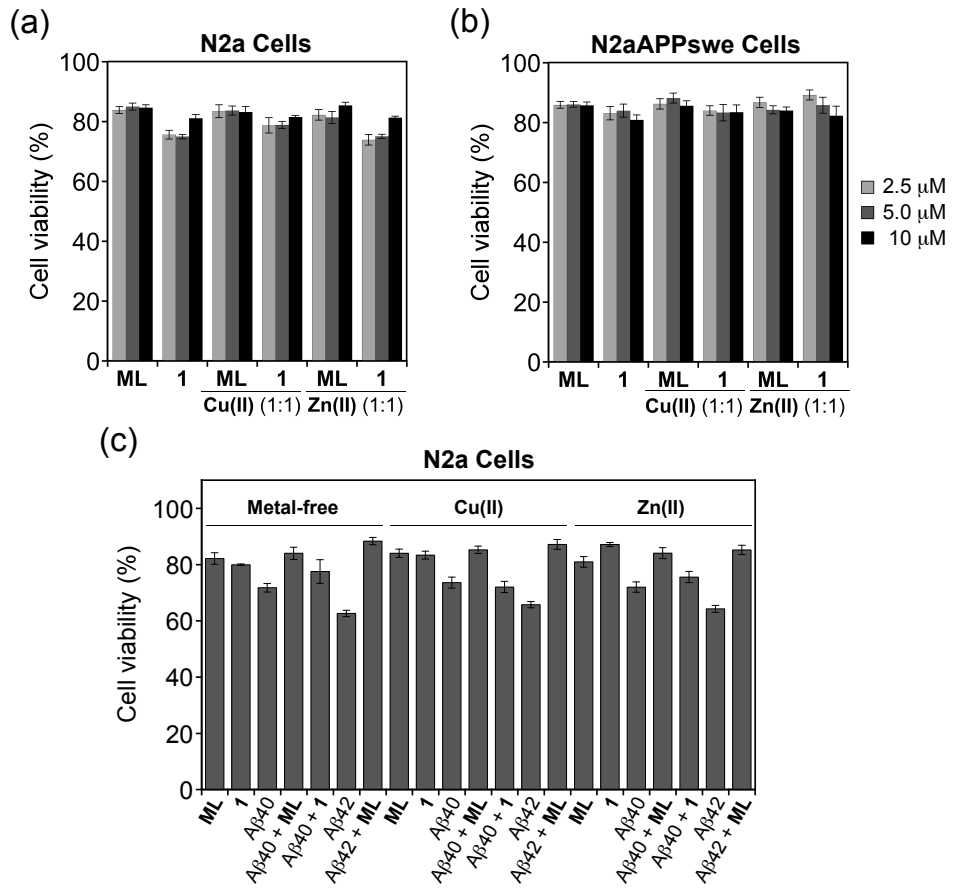

Figure S12. (a and b) Cytotoxicity study of **ML** or **1** in the absence and presence of Cu(II) or Zn(II) and (c) their modulation of toxicity caused by metal-free and metal-treated Aβ species in living cells. Cytotoxicity of **ML** or **1** in (a) murine Neuro-2a (N2a) neuroblastoma cells and (b) N2a cells overexpressing the Swedish mutant human amyloid precursor proteins (APP) (N2aAPPswe). Cells were treated with various concentrations of **ML** or **1** with/without a metal chloride salt ($CuCl_2$ or $ZnCl_2$) for 24 h at 37 °C. (c) The effect of **ML** or **1** on metal-free and metal-treated Aβ species in N2a cells. Cells treated with Aβ40 or Aβ42 (10 μM), a metal chloride salt ($CuCl_2$ or $ZnCl_2$; 10 μM), with/without **ML** or **1** (10 μM) were incubated for 24 h at 37 °C. Cell viability was determined by the MTT assay and the values of viability (%) were calculated compared to cells treated with DMSO only (0-1%, v/v). Data are mean ± S.E.M. $P < 0.05$, $n = 3$.

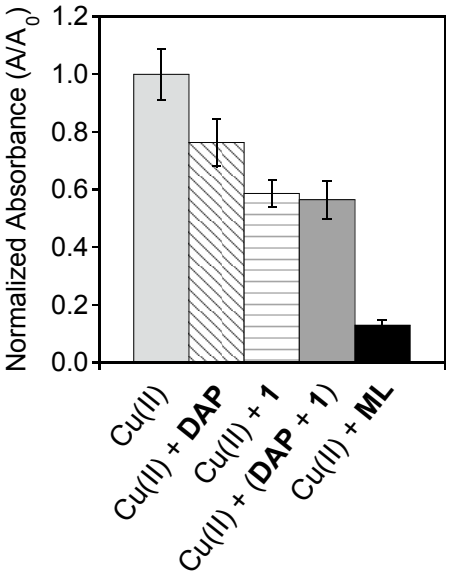

Figure S13. Inhibitory activity of **DAP**, **1**, and a mixture of **DAP** and **1** (**DAP** + **1**), relative to **ML**, toward ROS formation, determined by the 2-deoxyribose assay. The absorbance values are normalized compared to ligand-free condition ($CuCl_2$/compound = 10/125 μM). The conditions and methods are described in the Experimental Section.